JOURNAL OF NATURAL PRODUCTS

Article

Cite This: J. Nat. Prod. XXXX, XXX, XXX−XXX

pubs.acs.org/jnp

Izenamides A and B, Statine-Containing Depsipeptides, and an Analogue from a Marine Cyanobacterium

Yuki Kanamori,[†] Arihiro Iwasaki,[†] Shimpei Sumimoto,[†] Teruhiko Matsubara,[‡] Toshinori Sato,[‡] and Kiyotake Suenaga*[,†]

[†]Department of Chemistry, Faculty of Science and Technology, Keio University, 3-14-1 Hiyoshi, Ko-hoku-ku, Yokohama, Kanagawa 223-8522, Japan

[‡]Department of Biosciences and Informatics, Faculty of Science and Technology, Keio University, 3-14-1 Hiyoshi, Kohoku-ku, Yokohama, Kanagawa 223-8522, Japan

Supporting Information

ABSTRACT: Izenamides A, B, and C (**1**−**3**), new linear depsipeptides, were isolated from a taxonomically distinct marine cyanobacterium. Izenamides A and B contain a statine moiety [(3*S*,4*S*)-4-amino-3-hydroxy-6-methylheptanoic acid] and inhibited the activity of cathepsin D, an aspartic peptidase. Meanwhile, izenamides did not show growth-inhibitory activity against HeLa, HL60, or MCF-7 cells at up to 10 μM.

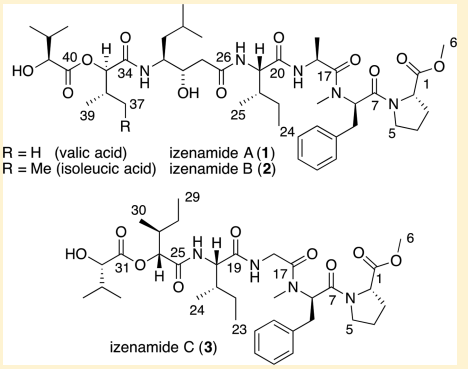

Marine cyanobacteria are precious sources of biologically active secondary metabolites. Among these metabolites, many peptides have been isolated from marine cyanobacteria and biosynthesized by nonribosomal peptide synthases (NRPS), polyketide synthases (PKS), and ribosomes. They are noteworthy not only because of their remarkable structures, such as unusual amino acid or fatty acid moieties, but also because of their biological activities.[1] Therefore, compounds from marine cyanobacteria can be expected to lead to the discovery of new drugs. In fact, several peptides possessing potent cytotoxicity, such as dolastatin 10,[2] apratoxin,[3] bisebromoamide,[4] and kurahyne,[5] have been discovered from marine cyanobacteria, and the new drug "brentuximab vedotin", which is used in the treatment of anaplastic large cell lymphoma and Hodgkin's lymphoma, was developed based on the structure of dolastatin 10.[6] Furthermore, some peptides derived from cyanobacteria are potent protease inhibitors, such as urumamide[7] (chymotrypsin), lyngbyastatins 4−10[8] (elastase), gallinamide A[9] (cathepsin L), and grassystatins A−F[10] (cathepsins D/E). Proteases have been recognized as pathogenic factors in many human diseases such as cancer,[11] Alzheimer's disease,[12] and HIV infection;[13] thus the therapeutic modulation of proteolytic activity by drugs may represent an approach to treatment.

Herein, we describe the isolation, structure determination, and biological evaluation of three linear depsipeptides, izenamides A−C (**1**−**3**), from a marine cyanobacterium. Izenamides A and B (**1** and **2**) are new inhibitors of cathepsin D and contain a statine moiety [(3*S*,4*S*)-4-amino-3-hydroxy-6-methylheptanoic acid, Sta].

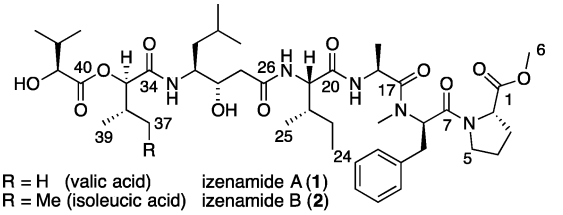

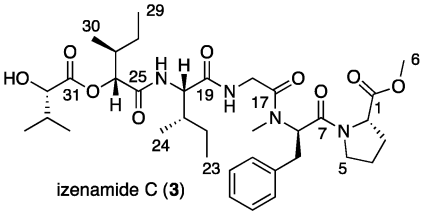

RESULTS AND DISCUSSION

The marine cyanobacterium 1605-5[14] (1700 g, wet weight) was collected at Izena Island, Okinawa, Japan. This sample was morphologically classified into *Lyngbya* (Figure S39). However, based on a 16S rRNA sequence analysis, the cyanobacterium was taxonomically distinct from the *Lyngbya* genus (Figure S40). The sample was extracted with MeOH. The extract was filtered, concentrated, and partitioned between EtOAc and H_2O. The EtOAc-soluble material was further partitioned

Received: May 24, 2018

Downloaded via UNIV OF CALIFORNIA SANTA BARBARA on June 27, 2018 at 03:11:50 (UTC).
See https://pubs.acs.org/sharingguidelines for options on how to legitimately share published articles.

ACS Publications

© XXXX American Chemical Society and American Society of Pharmacognosy

DOI: 10.1021/acs.jnatprod.8b00417
J. Nat. Prod. XXXX, XXX, XXX−XXX

Table 1. NMR Spectra for Izenamide A (1) at 400 MHz (^{1}H) and 100 MHz (^{13}C) in CD_3OD

residue	position	δ_C, type	δ_H, mult (J in Hz)	COSY	HMBC (H→C)	selected NOESY
Pro-*O*-Me	1	173.8,[a] C				
	2	60.9, CH	4.42, dd (7.4, 7.0)	3a, 3b	1, 3, 4	
	3a	30.0, CH_2	2.27, m	2, 3b, 4a, 4b	1, 2, 4, 5	
	3b		1.86, m	2, 3a, 4a	1, 2, 4, 5	
	4a	26.2, CH_2	1.96, m	3a, 3b, 4b, 5a, 5b	3	
	4b		1.86, m	3a, 4a, 5a, 5b	2, 3	
	5a	48.5, CH_2	3.46, m	4a, 4b, 5b	3, 4	8
	5b		3.40, m	4a, 4b, 5a	3, 4	
	6	52.6, CH_3	3.72, s		1	
N-Me-Phe	7	170.3, C				
	8	57.2, CH	5.70, dd (10.0, 5.8)	9a, 9b	7, 9, 10, 16, 17	5a
	9a	35.6, CH_2	3.11, dd (14.4, 5.8)	8, 9b	8, 10, 11/15	
	9b		2.93, dd (14.4, 10.0)	8, 9a	7, 8, 10, 11/15	
	10	138.3, C				
	11/15	130.8, CH	7.24, m		9, 10, 12/14, 13, 15/11	
	12/14	129.2, CH	7.24, m	13	10, 11/15, 13, 14/12	
	13	127.6, CH	7.16, m	12/14	11/15, 12/14	
	16	31.0, CH_3	3.07, s		8, 17	18
Ala	17	174.6, C				
	18	46.6, CH	4.69, q (7.0)	19	17, 19	16
	19	16.6, CH_3	0.82, d (7.0)	18	17, 18	
Ile	20	173.0, C				
	21	58.6, CH	4.21, d (7.4)	22	20, 22, 23, 25	27
	22	38.3, CH	1.76, m	21, 23a, 23b, 25	21, 23, 24, 25	
	23a	25.7, CH_2	1.49, m	22, 23b, 24	21, 25	
	23b		1.15, m	22, 23a, 24	21, 22, 24, 25	
	24	11.5, CH_3	0.87, t (7.4)	23a, 23b	22, 23	
	25	15.8, CH_3	0.87, d (7.0)	22	21, 22, 23	
Sta	26	173.9,[a] C				
	27	41.4,[b] CH_2	2.38, m	28	26, 28, 29	21
	28	71.3, CH	3.99, m	27	26, 27	
	29	52.2, CH	3.99, m	30a, 30b	34	
	30a	41.3,[b] CH_2	1.57, m	29, 30b	29, 31	
	30b		1.33, m	29, 30a	31	
	31	26.0, CH	1.56, m	32, 33	29, 30, 32	
	32	23.8, CH_3	0.93, d (6.1)	31	30, 31, 33	
	33	22.2, CH_3	0.89, d (6.3)	31	30, 31, 32	
valic acid-2	34	171.7, C				
	35	80.6, CH	4.72, d (5.8)	36	34, 36, 37, 40	
	36	31.7, CH	2.14, m	35, 37a, 38	34, 35, 37, 39	
	37a	18.1, CH_3	1.01, d (6.7)	36	35, 36, 39	
	37b					
	38					
	39	19.25,[c] CH_3	1.01, d (6.7)	36	35, 36, 37a	
valic acid-1	40	175.8, C				
	41	76.4, CH	4.13, d (4.5)	42	40, 42, 43, 44	
	42	33.3, CH	2.10, m	41, 43, 44	40, 41, 43, 44	
	43	19.30,[c] CH_3	1.01, d (6.7)	42	41, 42, 44	
	44	17.2, CH_3	0.93, d (6.7)	42	41, 42, 43	

[a−c]These signals are interchangeable.

between 90% aqueous MeOH and hexane to give an aqueous MeOH portion. This portion was subjected to fractionation with reversed-phase column chromatography (ODS silica gel, MeOH−H_2O) and repeated reversed-phase HPLC to give izenamides A (**1**, 34.0 mg), B (**2**, 2.2 mg), and C (**3**, 6.1 mg).

The molecular formula of izenamide A (**1**) was determined to be $C_{43}H_{69}N_5O_{11}$ based on HRESIMS data. Perusal of the ^{1}H and ^{13}C NMR spectra revealed that **1** was a depsipeptide (Table 1) with proton signals of one *N*-methyl amide substituent (δ_H 3.07), one *O*-methyl ester substituent (δ_H 3.72), α-protons (δ_H 4−5) of amides, aromatic protons (δ_H 7.1−7.3), and a methine adjacent to an acylated oxygen atom ($\delta_{H/C}$ 4.72/80.6). Further analyses of the ^{1}H NMR, ^{13}C NMR, COSY, HMQC, HMBC, and NOESY spectra in CD_3OD (Table 1) revealed the presence of a statine (Sta), four α-amino acid (Pro-*O*-Me, *N*-Me-Phe, Ala, and Ile), and two valic acid residues. Based on analyses of the HMBC and NOESY spectra, two structural fragments, [(valic acid-1)-(valic acid-2)-Sta-Ile] and [Ala-(*N*-Me-Phe)-(Pro-*O*-

DOI: 10.1021/acs.jnatprod.8b00417
J. Nat. Prod. XXXX, XXX, XXX−XXX

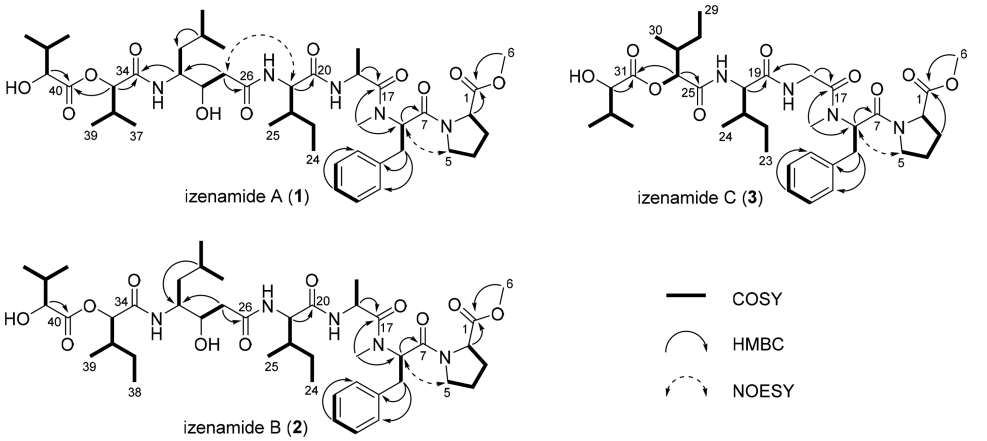

Figure 1. 2D NMR data for izenamides A–C (**1**–**3**).

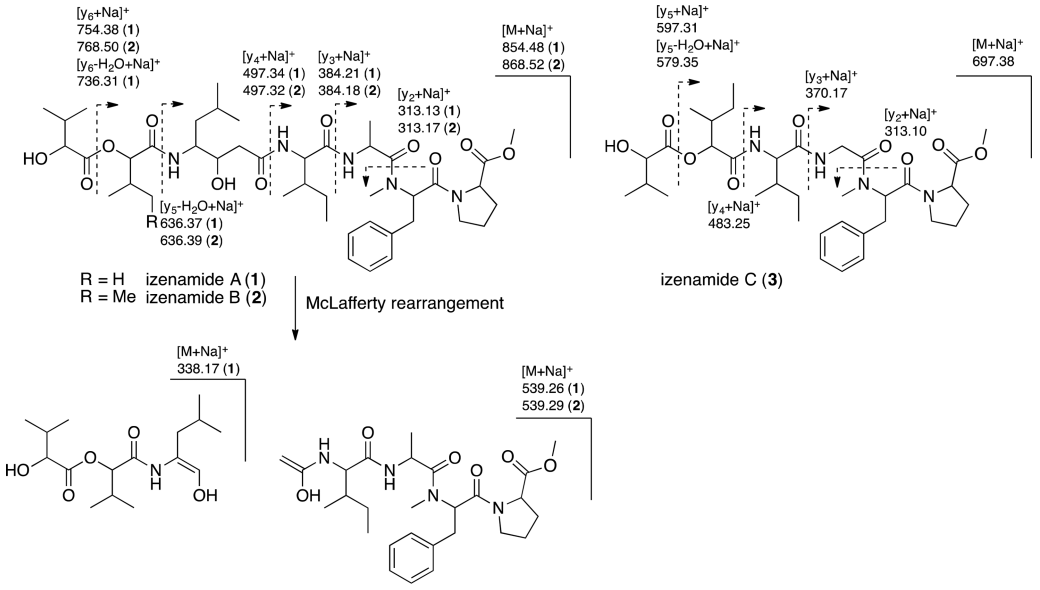

Figure 2. Selected MS fragmentation cleavages for izenamides A–C (**1**–**3**).

Me)], were established. The continuous sequence of these two fragments was clarified to be [(valic acid-1)-(valic acid-2)-Sta-Ile-Ala-(*N*-Me-Phe)-(Pro-*O*-Me)] by ESI-ion trap MS (ESI-ITMS) fragmentation analysis (Figures 1 and 2).

To establish the absolute configuration of **1**, the acid hydrolysate of **1** was analyzed by chiral-phase HPLC. The result revealed the presence of L-Ile, L-Ala, *N*-Me-D-Phe, L-Pro, and D/L-valic acid residues in izenamide A (**1**). To distinguish the D/L-valic acid residues, **1** was hydrolyzed under basic conditions, and we obtained the valic acid derived from the N-terminus of **1**.[14] Chiral-phase HPLC analysis for this valic acid determined that the N-terminal valic acid was the L-form. On the other hand, the other fragment without the L-valic acid residue was hydrolyzed under acidic conditions, and the hydrolysate was analyzed by chiral-phase HPLC. As expected, only D-valic acid was detected in this analysis. Regarding the Sta moiety, the absolute configuration of the hydroxy group at C-28 was determined to be *S* by a modified Mosher's method[15] (S43, Supporting Information). According to a previous paper, the relative configuration of a γ-amino-β-hydroxy acid, such as a Sta unit, can be easily determined by examination of the coupling constants and the ^{1}H NMR chemical shifts of the α-methylene signals.[16] In $CDCl_3$, the more deshielded α-proton signal (H-27a, δ_H 2.41, dd (J = 14.8, 8.8 Hz)) showed a large coupling to H-28, and the more shielded α-proton signal (H-27b, δ_H 2.35, dd (J = 14.8, 5.2 Hz)) showed a small coupling to H-28 (Table S1, Supporting Information). These observations indicated that the relative configuration was *anti* (Figure S32). Therefore, the absolute configuration of Sta in **1** was determined to be (3*S*, 4*S*), and the absolute configuration of izenamide A (**1**) was established as shown in formula 1.

The molecular formula of izenamide B (**2**) was determined to be $C_{44}H_{71}N_5O_{11}$ based on the HRESIMS data, which is larger than that of **1** by 14 MS units (CH_2). The ^{1}H and ^{13}C NMR spectra revealed that the structure of **2** was very similar to that of **1**. Further NMR analyses revealed all of the partial structures in **2**: Pro-*O*-Me, *N*-Me-Phe, Ala, Ile, valic acid, isoleucic acid, and Sta residues. Next, we determined their sequence based on NMR data (Table 2). The presence of the fragment [Ala-(*N*-Me-Phe)-(Pro-*O*-Me)] was determined on the basis of HMBC and NOESY data. The remaining sequence was clarified to be [valic acid-isoleucic acid-Sta-Ile-Ala-(*N*-Me-Phe)-(Pro-*O*-Me)] by ESI-ITMS fragmentation analysis (Figures 1 and 2).

To establish the absolute configuration, the acid hydrolysate of **2** was analyzed by chiral-phase HPLC. The result revealed the presence of L-Ile, L-Ala, *N*-Me-D-Phe, and L-Pro in **2**. However,

DOI: 10.1021/acs.jnatprod.8b00417
J. Nat. Prod. XXXX, XXX, XXX−XXX

Table 2. NMR Spectra for Izenamides B (2) and C (3) at 400 MHz (^{1}H) and 100 MHz (^{13}C) in CD_3OD

izenamide B (2)				izenamide C (3)			
residue	position	δ_C, type	δ_H, mult (J in Hz)	residue	position	δ_C, type	δ_H, mult (J in Hz)
Pro-*O*-Me	1	173.8,[a] C		Pro-*O*-Me-	1	174.0, C	
	2	61.0, CH	4.42, dd (7.0, 7.0)		2	60.6, CH	4.37, dd (8.8, 5.4)
	3a	30.0, CH_2	2.27, m		3a	29.9, CH_2	2.20, m
	3b		1.86, m		3b		1.85, m
	4a	26.2, CH_2	1.96, m		4a	26.0, CH_2	1.93, m
	4b		1.86, m		4b		1.85, m
	5a	48.5, CH_2	3.46, m		5a	48.1, CH_2	3.45, m
	5b		3.40, m		5b		3.40, m
	6	52.6, CH_3	3.72, s		6	52.7, CH_3	3.71, s
N-Me-Phe	7	170.4, C		*N*-Me-Phe	7	170.2,[c] C	
	8	57.2, CH	5.70, dd (10.0, 5.8)		8	57.8, CH	5.58, dd (7.6, 7.6)
	9a	35.6, CH_2	3.11, dd (14.4, 5.8)		9a	35.6, CH_2	3.19, dd (13.7, 7.6)
	9b		2.94, dd (14.4, 10.0)		9b		2.84, dd (13.7, 7.6)
	10	138.3, C			10	138.6, C	
	11/15	130.8, CH	7.24, m		11/15	130.5, CH	7.24, m
	12/14	129.2, CH	7.24, m		12/14	129.4, CH	7.24, m
	13	127.6, CH	7.16, m		13	127.6, CH	7.17, m
	16	31.0, CH_3	3.07, s		16	30.5, CH_3	3.03, s
Ala	17	174.6, C		Gly	17	170.1,[c] C	
	18	46.6, CH	4.68, q (7.0)		18a	41.9, CH_2	4.16, d (17.1)
	19	16.6, CH_3	0.83, d (7.0)		18b		3.91, d (17.1)
Ile	20	173.0, C		Ile	19	173.4, C	
	21	58.7, CH	4.21, d (7.4)		20	58.9, CH	4.34, d (7.0)
	22	38.3, CH	1.76, m		21	37.9, CH	1.92, m
	23a	25.7, CH_2	1.49, m		22a	25.7, CH_2	1.47, m
	23b		1.15, m		22b		1.14, m
	24	11.5, CH_3	0.87, t (7.4)		23	11.5, CH_3	0.89, dd (7.4, 7.4)
	25	15.8, CH_3	0.87, d (6.7)		24	16.1, CH_3	0.93, d (7.0)
Sta	26	173.9,[a] C		isoleucic acid	25	172.2, C	
	27	41.4,[b] CH_2	2.38, m		26	77.9, CH	5.07, d (4.5)
	28	71.4, CH	3.99, m		27	38.5, CH	1.94, m
	29	52.3, CH	3.99, m		28a	27.0, CH_2	1.44, ddq (13.9, 7.6, 7.6)
	30a	41.3,[b] CH_2	1.57, m		28b		1.29, ddq (13.9, 7.6, 7.6)
	30b		1.33, m		29	11.9, CH_3	0.96, t (7.6)
	31	26.0, CH	1.56, m		30	14.7, CH_3	0.96, d (7.0)
	32	23.8, CH_3	0.93, m	valic acid	31	175.1, C	
	33	22.2, CH_3	0.89, m		32	76.4, CH	4.12, d (4.3)
isoleucic acid	34	171.8, C			33	33.3, CH	2.11, qqd (7.0, 6.7, 4.3)
	35	78.3, CH	4.93, m		34	19.4, CH_3	1.01, d (7.0)
	36	40.2, CH	1.91, m		35	16.9, CH_3	0.91, d (6.7)
	37a	27.0, CH_2	1.45, m				
	37b		1.31, m				
	38	11.9, CH_3	0.96, m				
	39	14.8, CH_3	0.98, m				
valic acid	40	175.8, C					
	41	76.0, CH	4.14, d (4.5)				
	42	33.3, CH	2.10, m				
	43	19.3, CH_3	1.01, m				
	44	17.1, CH_3	0.92, m				

[a−c]These signals are interchangeable.

we could not clarify the absolute configurations of the two α-hydroxy acid moieties due to epimerization during acid hydrolysis. To prevent epimerization, **2** was hydrolyzed under basic conditions to give the valic acid, which was analyzed by chiral-phase HPLC and determined to be in the L-form. Meanwhile, chiral-phase HPLC analysis of the acid hydrolysate of the other fragment without the L-valic acid revealed the presence of D-*allo*-isoleucic acid in **2**. Regarding the Sta moiety, the relative configuration was determined to be *anti* based on the same analysis as described above (Table S1, Figure S32). To determine the absolute configuration at C-28, a modified Mosher's method was carried out. Although the (*R*)-MTPA ester of **2** was obtained as a single isomer, the (*S*)-MTPA ester was obtained as two diastereomers probably due to epimerization during the derivatization reaction.[17] Despite several attempts, epimerization could not be avoided. Therefore, we

DOI: 10.1021/acs.jnatprod.8b00417
J. Nat. Prod. XXXX, XXX, XXX−XXX

calculated $\Delta\delta$ ($\Delta\delta_{(S)\text{-MTPA}} - \Delta\delta_{(R)\text{-MTPA}}$) values by using each diastereomer of the (*S*)-MTPA esters, respectively. Fortunately, in both cases, the distributions of the positive and negative $\Delta\delta$ values were consistent with each other, which indicated that the absolute configuration at C-28 was *S* (S46). Therefore, the absolute configuration of Sta in **2** was determined to be (3*S*, 4*S*), the same configuration as that in **1**, and we clarified the structure of izenamide B (**2**).

The molecular formula of izenamide C (**3**) was determined to be $C_{35}H_{54}N_4O_9$ based on HRESIMS data. Detailed analyses of the ^{1}H NMR, ^{13}C NMR, COSY, HMQC, HMBC, and NOESY spectra in CD_3OD of **3** (Table 3) revealed the presence of one valic acid, one isoleucic acid, and four α-amino acid (Pro-*O*-Me, *N*-Me-Phe, Gly and Ile) residues. The sequence of **3** was clarified to be [valic acid-isoleucic acid-Ile-Gly-(*N*-Me-Phe)-(Pro-*O*-Me)] based on the HMBC and NOESY spectra (Figure 1). This assembly was corroborated by an ESI-ITMS fragmentation (Figure 2).

Table 3. IC_{50} Values of Izenamides A–C (1–3) against Cathepsin D

	IC_{50} values[b]
izenamide A (**1**)	380 ± 90 nM
izenamide B (**2**)	270 ± 150 nM
izenamide C (**3**)	>10 μM
pepstatin A[a]	50 ± 48 pM

[a]Positive control. [b]Values are shown ± SD.

To establish the absolute configuration, a portion of **3** was hydrolyzed under acidic conditions, and the hydrolysate was analyzed by chiral-phase HPLC. The result revealed the presence of L-valic acid, D-*allo*-isoleucic acid, L-Ile, *N*-Me-D-Phe, and L-Pro in **3**, and thus the absolute configuration of **3** was established.

The structures of izenamides A (**1**) and B (**2**) were similar to those of the known depsipeptides grassystatins[10] and tasiamides B and F.[18] These known compounds possess a γ-amino acid moiety as a common structure and have been known to inhibit some proteases such as cathepsin D. Although this unusual amino acid moiety is clarified to be responsible for the protease-inhibitory activity, detailed structure–activity relationship (SAR) studies beyond the γ-amino acid part are needed.

We assessed the biological activities of izenamides (**1**–**3**). First, we evaluated the cell-growth-inhibitory activity by MTT assay and found that **1**–**3** did not exhibit any cytotoxicity against HeLa, HL60, or MCF-7 cells up to 10 μM. Next, we focused on the characteristic γ-amino acid moiety, the Sta residue, in **1** and **2**. The Sta unit was first described as a partial structure of a very potent cathepsin D inhibitor, pepstatin A, from an *Actinomyces* sp.[19] The inhibitory mechanism of pepstatin A against cathepsin D was elucidated based on a cocrystal structure analysis, which found that the hydroxy group in a Sta unit interacts with the two aspartate residues in the active site of the enzyme, Asp33 and

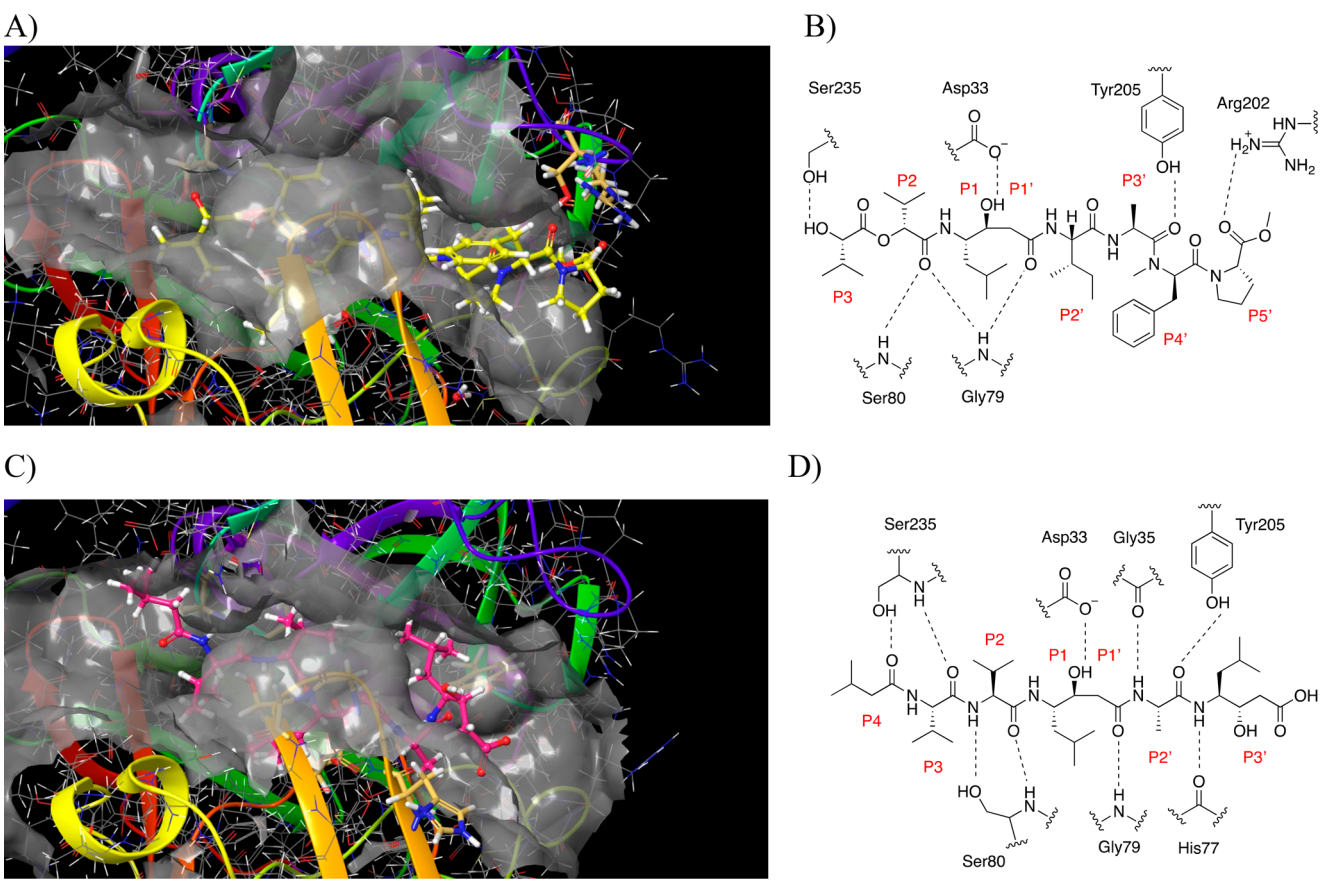

Figure 3. Conformational analyses of izenamide A (**1**)/cathepsin D and pepstatin A/cathepsin D. (A) Docking conformation of izenamide A (**1**, yellow) with cathepsin D in the global minimum energy. (B) Plausible hydrogen bonds between izenamide A (**1**) with cathepsin D in the global minimum energy. (C) Cocrystal structure of pepstatin A with cathepsin D (1LYB). (D) Plausible hydrogen bonds between pepstatin A with cathepsin D in the cocrystal, 1LYB.

DOI: 10.1021/acs.jnatprod.8b00417
J. Nat. Prod. XXXX, XXX, XXX–XXX

Asp231.[20] Cathepsin D, an aspartic endopeptidase, has attracted attention due to its association with several diseases. For example, cathepsin D is associated with cancer in that it promotes proliferation, invasion, and metastasis and is clinically used as a tumor marker of breast cancer.[21] In addition, it has been suggested that cathepsin D plays a significant role in the infection of humans by influenza viruses.[22] Therefore, the discovery of a new cathepsin D inhibitor is significant for the development of new drugs. Against this background, izenamides A−C (**1**−**3**) were subjected to a cathepsin D-inhibition assay. As expected, **1** and **2** exhibited similar potent inhibitory activities against cathepsin D. Compound **3**, without a Sta residue, did not show this activity (Table 3).

Compared with the IC_{50} values against cathepsin D, the activities of both **1** and **2** were much weaker than that of pepstatin A (Table 3), although they possessed a Sta unit. To elucidate the cause of this difference at the molecular level, we calculated a plausible docking structure of izenamide A (**1**) and cathepsin D using a molecular modeling method (MacroModel)[23] as follows. The crystal structure of cathepsin D with pepstatin A (1LYB) was used as a starting point. Based on the cocrystal structure, izenamide A (**1**) was manually docked into the pepstatin A-binding pocket on the enzyme. Next, we performed a conformational search for **1** and the amino acid residues around **1** by a torsional sampling method. As a constraint, the Sta moiety, which blocks the active site of cathepsin D, was placed within 4 Å from the active site of cathepsin D. Optimization of the obtained conformations afforded the docking pose in the global minimum energy (Figure 3A) along with those in several local energy minima. Considering the Boltzmann distribution at room temperature, we found that the conformation at the global minimum energy accounted for 93% of the total (Table S2). Therefore, we regarded this conformation to be the plausible docking pose of izenamide A (**1**) at the cathepsin D active site (Figure 3A).

Before starting detailed analyses of the docking structure, we validated our calculation approach as follows. We carried out molecular modeling of pepstatin A and cathepsin D by using the same method as described above and successfully regenerated the crystal structure of 1LYB (Figure S38). On the basis of this result, we confirmed the adequacy of this approach.

On the basis of the docking structure (Figure 3A) and the cocrystal structure (Figure 3C), we assessed several factors that affect the stability of the complex structures of izenamide A (**1**)/cathepsin D and pepstatin A/cathepsin D by MacroModel and found that two factors significantly destabilize the docking structure of **1** (Table S3).

The first destabilizing factor is the protrusion of a hydrophobic group into the hydrophilic environment. The C-terminal residue of pepstatin A (Figure 3C) is wrapped by the binding pocket of cathepsin D. On the other hand, regarding izenamide A (**1**) (Figure 3A), the hydrophobic methylene chain of Pro-*O*-Me protrudes into the solvent region (a water region). This unfavorable interaction could destabilize the ligand−receptor complex.

The second destabilizing factor is the difference in the hydrogen-bonding ability with the Ser80 residue between pepstatin A and izenamide A (**1**). We assessed the contribution of every hydrogen bond to stabilization of the ligand/receptor complex by using MacroModel (Figure 3B and D and Table S4). As a result, the stabilizing effect of the hydrogen bond from Ser80 was especially different between pepstatin A and izenamide A (**1**). While pepstatin A formed two hydrogen bonds with the Ser residue, **1** formed only one hydrogen bond with it. We analyzed the reason for this difference. The carbonyl group and amide-NH group of valine at the P2 residue in pepstatin A each formed a hydrogen bond with the Ser80 residue (Figure 3D). However, **1** possessed valic acid at the corresponding position instead of valine and could not form two hydrogen bonds with Ser80, probably due to the lack of an amide-NH (Figure 3B).

On the basis of these considerations, we conjectured the origin of the difference in the cathepsin D-inhibitory activity between **1** and pepstatin A. To date, a SAR study of cathepsin D and Sta-containing acyclic peptides has only been carried out using grassystatins.[10] Grassystatins were isolated from marine cyanobacteria and were shown to exhibit cathepsin D-inhibitory activity. They possess a hydrophilic amino acid residue at the P2 position, and the previous study clarified that this hydrophilicity reduces the affinity toward cathepsin D. Furthermore, it has been suggested that the presence of a *N*,*N*-dimethyl amino acid residue at the N-terminus potentiates the inhibitory activity. Our study on izenamides (**1**−**3**) adds new insights to the SAR study of cathepsin D and Sta-containing peptides.

In summary, we have reported the isolation and the structure determination of new linear depsipeptides, izenamides A−C (**1**−**3**), from a marine cyanobacterium collected at Okinawa, Japan. According to our identification study, this cyanobacterium is taxonomically independent of cyanobacteria in other genera including izenamide-analogue-producing cyanobacteria (Figure S40). The structures of **1**−**3** were elucidated by a combination of spectroscopic analyses and degradation/derivatization reactions. Izenamides A (**1**) and B (**2**), which possess a Sta moiety, inhibited cathepsin D without exhibiting cytotoxicity against HeLa, HL60, or MCF-7 cells. The cathepsin D-inhibitory activities of **1** and **2** were much weaker than that of pepstatin A, a structurally related known inhibitor. On the basis of a molecular modeling method, we suggested a cause for this difference at the molecular level. Recently, cathepsin D has attracted attention due to its association with several diseases, and this study provides new knowledge for the development of cathepsin D inhibitors.

EXPERIMENTAL SECTION

General Experimental Procedures. Optical rotations were measured with a JASCO DIP-1000 polarimeter. IR spectra were recorded on a JASCO FT/IR-4200 instrument. All NMR data were recorded on a JEOL JNM-ECX400 spectrometer for ^1H (400 MHz) and ^{13}C (100 MHz). ^1H NMR chemical shifts (referenced to residual CHD_2OD observed at δ_H 3.31 and $CHCl_3$ observed at δ_H 7.26) were assigned using a combination of data from COSY and HMQC experiments. Similarly, ^{13}C NMR chemical shifts (referenced to CD_3OD observed at δ_C 49.00 and $CDCl_3$ observed at δ_C 77.16) were assigned based on HMBC and HMQC experiments. HRESIMS spectra were obtained on an LCT Premier XE time-of-flight (TOF) mass spectrometer (LCT Premier XE, Waters). ESI-ITMS spectra were recorded with an amaZone SL mass spectrometer (Bruker Daltonics). Chromatographic analyses were performed using an HPLC system consisting of a pump (model PU-2080, JASCO) and a UV detector (model UV-2075, JASCO). All chemicals and solvents used in this study were the best grade available (special grade) from a commercial source.

Identification of the Marine Cyanobacterium. Small pieces of the collected marine cyanobacterium, 1605-5, were preserved for genetic analysis in RNA*later* (Qiagen). To remove the cyanobacterial sheaths, the cyanobacterial sample was treated with 0.1% (w/v) sarkosyl solution before the isolation of single filaments. Single filaments of marine cyanobacteria were isolated by the pipet-washing

DOI: 10.1021/acs.jnatprod.8b00417
J. Nat. Prod. XXXX, XXX, XXX−XXX

method[24] under a light microscope. The isolated single filament was crushed with a pipet on a slide glass under a light microscope and dissolved in 10 μL of sterilized H_2O. The sterilized H_2O containing the broken filament was used as a DNA template for PCR amplification.

The 16S rRNA genes were PCR-amplified in two stages by using two cyanobacterial primer sets: CYA 106F[25] and 23S 30R[26] for the first amplification, and CYA 359F[25] and 16S 1371R[27] for the second amplification. The first PCR reaction contained 10 μL of DNA template, 0.5 μL of KOD-Multi & Epi- (Toyobo), 12.5 μL of 2× PCR buffer for KOD-Multi & Epi- (Toyobo), and 1.0 μL of CYA 106F and 23S 30R (10 pM). The PCR reaction was carried out with a T100 thermal cycler (Bio-Rad) as follows: initial denaturation at 94 °C for 2 min, amplification for 40 cycles of 10 s at 98 °C, and final elongation at 66 °C for 1.5 min. The obtained PCR products were diluted 1000-fold with sterilized H_2O. The second PCR reaction contained 10 μL of the diluted PCR product, 0.5 μL of KOD-Multi & Epi- (Toyobo), 12.5 μL of 2× PCR buffer for KOD-Multi & Epi- (Toyobo), and 1.0 μL of CYA 359F and 16S 1371R (10 pM). The second PCR reaction was performed under the same conditions as the first PCR.

PCR products were analyzed on agarose gel (1%) in TBE buffer, visualized by ethidium bromide staining, and purified by a PCR Advanced PCR cleanup system (Viogene). Sequences were determined with CYA 359F and 16S 1371R primers by a commercial firm (Macrogen Japan Corp.). These sequences are available in the DDBJ/EMBL/GenBank databases under accession number LC315181.

Morphological Characterization. Morphological observation was performed using a phase contrast microscope (Eclipse Ti-S, Nikon). The mean cell size and standard deviation of 50 cells were measured. The cell length was 1.7 ± 0.5 μm, and the width was 17.3 ± 0.6 μm. The mean sheath size and standard deviation of 25 sheaths were measured. The thickness of the sheath was 1.2 ± 0.2 μm. The filaments were unbranched and the sheaths contained only one trichome, which were consistent with the morphological features of *Lyngbya*. The cell color was olive-green, and the sheath was colorless and unlamellated.

Morphologically, the cyanobacterium was very close to *Lyngbya confervoide*. However, although the sheath of *L. confervoide* is lamellated,[28] that of 1605-5 was not. 1605-5 was compared with *Okeania*,[29] *Moorea*[30] and *Caldora penicillata*,[31] but was not consistent with any of these genera (Table S5, Figure S39).

Phylogenetic Analysis. The nucleotide sequence of the 16S rRNA gene obtained in this study was used for phylogenetic analysis with the sequences of related cyanobacterial 16S rRNA genes that have been previously reported. All sequences were aligned by MEGA7[32] with a default setting of ClustalW. Gaps in the alignment data were manually deleted from the sequences, and 188 nucleotides were used for cladistics analysis. JModeltest (version 2.1.7)[33,34] with the default settings was used to select the best model of DNA substitution for the maximum likelihood (ML) analysis and Bayesian analysis according to the Akaike information criterion. The ML analysis was performed with RAxML[35] (version 8), using the GTR+I+G model. Bootstrap resampling was performed on 1000 replicates. The ML tree was visualized with Njplot (version 2.3).[36] The Bayesian analysis was conducted with MrBayes (version 3.2.6)[37] using the GTR+I+G model. The Markov chain Monte Carlo process was set at two chains, and 5 000 000 generations were conducted. The sampling frequency was assigned to be every 500 generations. After analysis, the first 500 000 trees were deleted as burn-in, and the consensus tree was constructed. The Bayesian tree was visualized with FigTree (version 1.4.3, http://tree.bio.ed.ac.uk/software/figtree/).

Collection, Extraction, and Isolation. The cyanobacterium 1605-5 was collected at Izena Island, Okinawa Prefecture, Japan, at a depth of 0−1 m in May 2016. The collected cyanobacterium (1700 g, wet weight) was extracted twice with MeOH (3 L). The extract was filtered and concentrated. The residue was partitioned between EtOAc (3 × 300 mL) and H_2O (500 mL). The material obtained from the organic layer was partitioned between hexane (3 × 300 mL) and 90% aqueous MeOH (300 mL) to give an aqueous MeOH fraction (1.39 g). This fraction was separated by column chromatography on ODS gel (Cosmosil 75C_{18}-OPN 14.0 g) eluting with 40% aqueous MeOH, 60% aqueous MeOH, 80% aqueous MeOH, MeOH, and $CHCl_3$−MeOH (1:1). The 80% MeOH fraction (450 mg) was subjected to HPLC [conditions for HPLC separation, Cosmosil 5C_{18}-AR-II (ϕ 20 mm × 250 mm); solvent 80% MeOH; flow rate 5 mL/min; detection UV 215 nm] in 12 batches to give several fractions containing izenamide C (**3**, 29.9 mg, t_R = 26.3 min), izenamide A (**1**, 52.3 mg, t_R = 29.1 min), and izenamide B (**2**, 67.4 mg, t_R = 36.0 min). These fractions containing izenamides A−C were further separated by HPLC [Cosmosil Cholester (ϕ 20 mm × 250 mm); solvent 51% MeCN; flow rate 5 mL/min; detection UV 215 nm] in two batches to give izenamide A (**1**, 34.0 mg, t_R = 49.8 min), HPLC [Cosmosil Cholester (ϕ 20 mm × 250 mm); solvent 59% MeCN; flow rate 5 mL/min; detection UV 215 nm] in one batch to give izenamide B (**2**, 1.9 mg, t_R = 36.8 min), and HPLC [Cosmosil Cholester (ϕ 20 mm × 250 mm); solvent 55% MeCN; flow rate 5 mL/min; detection UV 215 nm] in one batch to give izenamide C (**3**, 6.1 mg, t_R = 38.2 min).

Izenamide A (1): colorless oil; $[\alpha]^{23}_D$ −17 (*c* 0.31, MeOH); IR (neat) ν_{max} 3316, 2962, 2875, 1746, 1632, 1537, 1453, 1367, 1265, 1198, 1034, 753 cm^{-1}; ^1H NMR, ^{13}C NMR, COSY, HMQC, HMBC, and selected NOESY data in CD_3OD, Table 1; ^1H NMR, COSY, and TOCSY in $CDCl_3$, Table S1; HRESIMS *m/z* 832.5048 $[M + H]^+$ (calcd for $C_{43}H_{70}N_5O_{11}$, 832.5072).

Izenamide B (2): colorless oil; $[\alpha]^{23}_D$ −11 (*c* 0.11, MeOH); IR (neat) ν_{max} 3313, 2962, 1743, 1633, 1533, 1446, 1198 cm^{-1}; ^1H NMR, ^{13}C NMR data, Table 2; ^1H NMR, COSY, and TOCSY in $CDCl_3$, Table S1; HRESIMS *m/z* 846.5237 $[M + H]^+$ (calcd for $C_{44}H_{72}N_5O_{11}$, 846.5228).

Izenamide C (3): colorless oil; $[\alpha]^{23}_D$ +24 (*c* 0.21, MeOH); IR (neat) ν_{max} 3313, 2964, 2877, 1746, 1635, 1521, 1446, 1199, 1177, 1135, 1031, 753 cm^{-1}; ^1H NMR, ^{13}C NMR data, Table 2; HRESIMS *m/z* 675.3956 $[M + H]^+$ (calcd for $C_{35}H_{55}N_4O_9$, 675.3970).

Determination of the Configuration of Izenamide A (1). Izenamide A (**1**, 0.2 mg) was dissolved in 100 μL of 9 M HCl in a sealed tube and heated at 110 °C for 24 h. The hydrolyzed products were evaporated to dryness and could be separated into each component by HPLC [conditions for HPLC separation: column, Cosmosil 5C_{18}- PAQ (ϕ 4.6 × 250 mm); flow rate, 1.0 mL/min; detection at 215 nm; solvent H_2O]. Retention times (t_R min) of components: Ala (2.9), Pro (3.3), Ile (4.6), *N*-Me-Phe (12.7).

Izenamide A (**1**, 0.2 mg) was dissolved in 150 μL of MeOH−0.5 M NaOH (1:1) and reacted at room temperature for 20 min. The solution was neutralized by the addition of 37.5 μL of 1 M HCl. The product was evaporated to dryness and separated to obtain the terminal valic acid (valic acid-1) by HPLC [conditions for HPLC separation: column, PBr (ϕ 4.6 × 250 mm); flow rate, 1.0 mL/min; detection at 215 nm; solvent MeCN−H_2O−trifluoroacetic acid (TFA) (5:95:0.1)]. Retention time (t_R min) of component: valic acid (10.8)]. The other product without the terminal residue was dissolved in 100 μL of 9 M HCl in a sealed tube and heated at 110 °C for 24 h. The hydrolyzed products were evaporated to dryness and separated to obtain another valic acid (valic acid-2) [conditions for HPLC separation: column, PBr (ϕ 4.6 × 250 mm); flow rate, 1.0 mL/min; detection at 215 nm; solvent MeCN−H_2O−TFA (5:95:0.1)]. Retention time (t_R min) of component: valic acid (11.9).

The configurations of the amino and hydroxy acids in **1** were determined by chiral-phase HPLC [DAICEL CHIRALPAK (MA+) (ϕ 4.6 × 50 mm); flow rate, 1.0 mL/min; detection at 254 nm; solvent 2.0 mM $CuSO_4$, 2.0 mM $CuSO_4$−MeCN (90:10), 2.0 mM $CuSO_4$−MeCN (85:15)]. With 2.0 mM $CuSO_4$ as a solvent, the retention times of Ala, Pro, and Ile matched those of the authentic standards of L-Ala (2.0 min; D-Ala, 1.6 min), L-Pro (6.3 min; D-Pro, 3.3 min), L-Ile (23.9 min; D-*allo*-Ile, 8.6 min, D-Ile, 11.0 min, L-*allo*-Ile, 16.8 min). With 2.0 mM $CuSO_4$−MeCN (90:10) as a solvent, the retention times of *N*-Me-Phe matched those of the authentic standards of *N*-Me-D-Phe (7.3 min; *N*-Me-L-Phe, 8.2 min). With 2.0 mM $CuSO_4$−MeCN (85:15) as a solvent, the retention times of the terminal valic acid-1 and valic acid-2 matched those of the authentic standards of L-valic acid (9.3 min; D-valic acid, 6.1 min) and D-valic acid, respectively.

To a stirred solution of izenamide A (**1**) (0.8 mg, 0.96 μmol) in pyridine (100 μL) were added 2 drops of (*R*)-MTPACl and 4-(dimethylamino)pyridine (0.3 mg, 2.5 μmol). The mixture was stirred

DOI: 10.1021/acs.jnatprod.8b00417
J. Nat. Prod. XXXX, XXX, XXX−XXX

at room temperature (rt) for 22 h and concentrated to give an oil, which was purified by HPLC [conditions for HPLC separation: column, Cosmosil 5C_{18}-MS-II (ϕ 4.6 × 250 mm); flow rate, 5.0 mL/min; detection at 215 nm; solvent MeOH−H_2O (90:10); t_R = 36.3 min] to afford the (*S*)-MTPA ester of **1** (0.5 mg) as a colorless oil: HRESIMS *m*/*z* 1264.5901 $[M + H]^+$ (calcd for $C_{63}H_{84}F_6N_5O_{15}$, 1264.5868).

To a stirred solution of **1** (1.3 mg, 1.6 μmol) and 4-(dimethylamino)pyridine (0.2 mg, 1.6 μmol) in pyridine (100 μL) were added 2 drops of (*S*)-MTPACl. The mixture was stirred at rt for 6 h and concentrated to give an oil, which was purified by HPLC [conditions for HPLC separation: column, Cosmosil 5C_{18}-AR-II (ϕ 4.6 × 250 mm); flow rate, 5.0 mL/min; detection at 215 nm; solvent MeOH−H_2O (90:10); t_R = 35.2 min] to afford the (*R*)-MTPA ester of **1** (0.9 mg) as a colorless oil: HRESIMS *m*/*z* 1264.5862 $[M + H]^+$ (calcd for $C_{63}H_{84}F_6N_5O_{15}$, 1264.5868).

Determination of the Configuration of Izenamide B (2). Izenamide B (**2**, 0.5 mg) was dissolved in 100 μL of 9 M HCl in a sealed tube and heated at 110 °C for 24 h. The hydrolyzed products were evaporated to dryness and could be separated into each component by HPLC [conditions for HPLC separation: column, Cosmosil 5C_{18}- PAQ (ϕ 4.6 × 250 mm); flow rate, 1.0 mL/min; detection at 215 nm; solvent H_2O]. Retention times (t_R min) of components: Ala (2.9), Pro (3.4), Ile (4.5), *N*-Me-Phe (12.6).

Izenamide B (**2**, 0.2 mg) was dissolved in 150 μL of MeOH−0.5 M NaOH (1:1) and reacted at rt for 20 min. The solution was neutralized by the addition of 37.5 μL of 1 M HCl. The product was evaporated to dryness and separated to obtain the terminal valic acid by HPLC [conditions for HPLC separation: column, PBr (ϕ 4.6 × 250 mm); flow rate, 1.0 mL/min; detection at 215 nm; solvent MeCN−H_2O−TFA (5:95:0.1)]. Retention time (t_R min) of component: valic acid (10.9). The product with the terminal residue removed was dissolved in 100 μL of 6 M HCl in a sealed tube and heated at 110 °C for 24 h. The hydrolyzed products were evaporated to dryness and separated to obtain isoleucic acid [conditions for HPLC separation: column, ODS HG-5 (ϕ 4.6 × 250 mm); flow rate, 1.0 mL/min; detection at 215 nm; solvent MeCN−H_2O−TFA (15:85:0.1)]. Retention time (t_R min) of component: isoleucic acid (12.0).

The configurations of the amino and hydroxy acids in **2** were determined by chiral-phase HPLC [DAICEL CHIRALPAK (MA+) (ϕ 4.6 × 50 mm); flow rate, 1.0 mL/min; detection at 254 nm; solvent 2.0 mM $CuSO_4$, 2.0 mM $CuSO_4$−MeCN (90:10), 2.0 mM $CuSO_4$−MeCN (85:15)]. With 2.0 mM $CuSO_4$ as a solvent, the retention times of Ala, Pro, and Ile matched those of the authentic standards of L-Ala (2.3 min; D-Ala, 1.7 min), L-Pro (7.2 min; D-Pro, 3.7 min), and L-Ile (23.9 min; D-*allo*-Ile, 8.6 min, D-Ile, 11.0 min, L-*allo*-Ile, 16.8 min). With 2.0 mM $CuSO_4$−MeCN (90:10) as a solvent, the retention times of *N*-Me-Phe matched those of authentic standards of *N*-Me-D-Phe (9.3 min; *N*-Me-L-Phe, 10.4 min). With 2.0 mM $CuSO_4$−MeCN (85:15) as a solvent, the retention times of valic acid and isoleucic acid matched those of authentic standards of L-valic acid (9.4 min; D-valic acid, 6.2 min) and D-*allo*-isoleucic acid (12.3 min; D-isoleucic acid, 14.4 min, L-*allo*-isoleucic acid, 18.8 min, L-isoleucic acid, 23.2 min).

To a stirred solution of izenamide B (**2**) (0.3 mg, 0.36 μmol) in pyridine (100 μL) were added 1 drop of (*R*)-MTPACl and 4-(dimethylamino)pyridine (0.1 mg, 0.82 μmol). The mixture was stirred at rt for 24 h and concentrated to give an oil, which was purified by HPLC [conditions for HPLC separation: column, Cosmosil 5C_{18}-MS-II (ϕ 4.6 × 250 mm); flow rate, 5.0 mL/min; detection at 215 nm; solvent MeOH−H_2O (90:10); t_R = 42.6, 43.5 min] to afford two kinds of (*S*)-MTPA esters of **2** (A, 0.3 mg; B, 0.2 mg, respectively) as colorless oils: HRESIMS *m*/*z* 1300.5841 for A, 1300.5851 for B $[M + Na]^+$ (calcd for $C_{64}H_{85}F_6N_5O_{15}Na$, 1300.5844).

To a stirred solution of **2** (0.3 mg, 0.36 μmol) in pyridine (100 μL) were added 1 drop of (*S*)-MTPACl and 4-(dimethylamino)pyridine (0.1 mg, 0.82 μmol). The mixture was stirred at rt for 24 h and concentrated to give an oil, which was purified by HPLC [conditions for HPLC separation: column, Cosmosil 5C_{18}-MS-II (ϕ 4.6 × 250 mm); flow rate, 5.0 mL/min; detection at 215 nm; solvent MeOH−H_2O (90:10); t_R = 40.2 min] to afford the (*R*)-MTPA ester of **2** (0.3 mg) as a colorless oil: HRESIMS *m*/*z* 1300.5844 $[M + Na]^+$ (calcd for $C_{64}H_{85}F_6N_5O_{15}Na$, 1300.5844).

Determination of the Configuration of Izenamide C (3). Izenamide C (**3**, 0.7 mg) was dissolved in 100 μL of 9 M HCl in a sealed tube and heated at 110 °C for 24 h. The hydrolyzed products were evaporated to dryness and could be separated into each component by HPLC. Conditions for HPLC separation: column, Cosmosil 5C_{18}-PAQ (ϕ 4.6 × 250 mm); flow rate, 1.0 mL/min; detection at 215 nm; solvent H_2O. Retention times (t_R min) of components: Pro (3.3), Ile (4.7), *N*-Me-Phe (12.4). Conditions for HPLC separation: column, PBr (ϕ 4.6 × 250 mm); flow rate, 1.0 mL/min; detection at 215 nm; solvent MeCN−H_2O−TFA (5:95:0.1). Retention time (t_R min) of component: valic acid (10.6). Conditions for HPLC separation: column, ODS HG-5 (ϕ 4.6 × 250 mm); flow rate, 1.0 mL/min; detection at 215 nm; solvent MeCN−H_2O−TFA (15:85:0.1). Retention time (t_R min) of component: isoleucic acid (13.1).

The configurations of the amino and hydroxy acids in **3** were determined by chiral-phase HPLC [DAICEL CHIRALPAK (MA+) (ϕ 4.6 × 50 mm); flow rate, 1.0 mL/min; detection at 254 nm; solvent 2.0 mM $CuSO_4$, 2.0 mM $CuSO_4$−MeCN (90:10), 2.0 mM $CuSO_4$−MeCN (85:15)]. With 2.0 mM $CuSO_4$ as a solvent, the retention times of Pro and Ile matched those of authentic standards of L-Pro (5.1 min; D-Pro, 2.8 min) and L-Ile (16.6 min; D-*allo*-Ile, 6.7 min, D-Ile, 8.4 min, L-*allo*-Ile, 12.2 min). With 2.0 mM $CuSO_4$−MeCN (90:10) as a solvent, the retention times of *N*-Me-Phe and valic acid matched those of authentic standards of *N*-Me-D-Phe (7.3 min; *N*-Me-L-Phe, 8.2 min) and L-valic acid (17.6 min; D-valic acid, 11.3 min). With 2.0 mM $CuSO_4$−MeCN (85:15) as a solvent, the retention times of isoleucic acid matched those of authentic standards of D-*allo*-isoleucic acid (14.1 min; D-isoleucic acid, 16.4 min, L-*allo*-isoleucic acid, 21.3 min, L-isoleucic acid, 26.1 min).

Cell Growth Inhibition Assay. HeLa and MCF-7 cells were cultured at 37 °C with 5% CO_2 in Dulbecco's modified Eagle's medium (Nissui) supplemented with 10% heat-inactivated fetal bovine serum (FBS), 100 units/mL penicillin, 100 μg/mL streptomycin, 0.25 μg/mL amphotericin, 300 μg/mL L-glutamine, and 2.25 mg/mL $NaHCO_3$. HL60 cells were cultured at 37 °C with 5% CO_2 in RPMI (Nissui) supplemented with 10% heat-inactivated FBS, 100 units/mL penicillin, 100 μg/mL streptomycin, 0.25 μg/mL amphotericin, 300 μg/mL L-glutamine, and 2.25 mg/mL $NaHCO_3$. HeLa and MCF-7 cells were seeded at 4 × 10^3 cells/well in 96-well plates (Iwaki) and cultured overnight. HL60 cells were seeded at 2 × 10^4 cells/well in 96-well plates. Ten and 1 μM of compounds **1**−**3** in methanol were then added, and cells were incubated for 72 h. Cell proliferation was measured by the MTT assay.

Cathepsin D Inhibition Assay. Cathepsin D-inhibitory activities of izenamides A−C (**1**−**3**) were assessed using a commercial assay kit provided by Biovision (#K148-100) according to the manufacturer's protocol. The assay was attempted at the following concentrations: 1000, 100, 10 nM (**1** and **2**, *n* = 3), 10, 1, 0.1 μM (**3**, *n* = 3), and 250, 25, 2.5 pM (pepstatin A, *n* = 2).

Molecular Modeling of Izenamide A (1) with Cathepsin D. The molecular modeling of izenamide A (**1**) and cathepsin D was carried out using MacroModel (version 11.3).[24] The crystal structure of cathepsin D with pepstatin A (PDB: 1LYB) was used as a starting point. Based on the cocrystal structure, izenamide A (**1**) was manually docked into the binding pocket of cathepsin D, and the hydroxy group in the Sta unit in **1**, which was expected to interact with the active site of the enzyme, was placed within 4 Å of the two aspartate residues in the active site, Asp33 and Asp231.[21] Torsional sampling by the Monte Carlo Multiple Minimum method (1000 steps) was used to perform a conformational search, and the obtained complex was minimized using an OPLS3 force field and the Polak−Ribier conjugate gradient algorithm (maximum derivative less than 0.1 kJ/mol) with water as a solvent. To perform a conformational search, all bonds in izenamide A (**1**) and amino acid residues within 3 Å of **1** were considered as torsional sampling targets, except for amide bonds. In addition, residues within 6 Å of the ligand were set to be free, those between 6 and 10 Å were constrained by a force of 200 kJ/(mol·$Å^2$), and those between 10 and 20 Å were set to be frozen. To select nonredundant conformers, we

DOI: 10.1021/acs.jnatprod.8b00417
J. Nat. Prod. XXXX, XXX, XXX−XXX

eliminated redundant conformers by setting a 1.0 Å root-mean-square deviation minimum cutoff for saving structure. To validate our calculation approach, we carried out the same calculation for the complex of pepstatin A and cathepsin D and successfully regenerated the structure of 1LYB (Figure S38). The Boltzmann distribution of the obtained conformations was calculated by MacroModel (Table S2). The factors that affected the stability of the ligand/receptor complex were analyzed based on the results of the calculation using XP (extra precision) mode (Table S3). The contribution of each amino acid residue to stabilization of the complex was estimated based on the results of the same calculation (Table S4). The hydrogen bonds were defined as having donor−acceptor distances within 2.5 Å from the protein to the inhibitor.

■ ASSOCIATED CONTENT

Supporting Information

The Supporting Information is available free of charge on the ACS Publications website at DOI: 10.1021/acs.jnatprod.8b00417.

NMR spectra and MS/MS spectra for all new compounds; determination of the absolute configuration of izenamides A, B, and C; molecular modeling of pepstatin A and cathepsin D; identification of the cyanobacterium (PDF)

■ AUTHOR INFORMATION

Corresponding Author

*E-mail: suenaga@chem.keio.ac.jp. Tel: +81-45-566-1819.

ORCID

Arihiro Iwasaki: 0000-0002-3775-5066
Teruhiko Matsubara: 0000-0002-8006-4324
Toshinori Sato: 0000-0002-4429-6101
Kiyotake Suenaga: 0000-0001-5343-5890

Notes

The authors declare no competing financial interest.

■ ACKNOWLEDGMENTS

This work was supported in part by Grants-in-Aid from the Ministry of Education, Culture, Sports, Science and Technology of Japan (16H03285 and 17H05450) and Keio Leading-edge Laboratory of Science, and Technology (KLL)-specified research projects.

■ REFERENCES

(1) Shah, S. A. A.; Akhter, N.; Auckloo, B. N.; Khan, I.; Lu, Y.; Wang, K.; Wu, B.; Guo, Y. W. *Mar. Drugs* **2017**, *15*, 354−383.

(2) (a) Pettit, G. R.; Kamano, Y.; Herald, C. L.; Tuinman, A. A.; Boettner, F. E.; Kizu, H.; Schmidt, J. M.; Baczynskyj, L.; Tomer, K. B.; Bontems, R. J. *J. Am. Chem. Soc.* **1987**, *109*, 6883−6885. (b) Luesch, H.; Moore, R. E.; Paul, V. J.; Mooberry, S. L.; Corbett, T. H. *J. Nat. Prod.* **2001**, *64*, 907−910.

(3) Luesch, H.; Yoshida, W. Y.; Moore, R. E.; Paul, V. J.; Corbett, T. H. *J. Am. Chem. Soc.* **2001**, *123*, 5418−5423.

(4) Teruya, T.; Sasaki, H.; Fukazawa, H.; Suenaga, K. *Org. Lett.* **2009**, *11*, 5062−5065.

(5) Iwasaki, A.; Ohno, O.; Sumimoto, S.; Suda, S.; Suenaga, K. *RSC Adv.* **2014**, *4*, 12840−12843.

(6) Senter, P. D.; Sievers, E. L. *Nat. Biotechnol.* **2012**, *30*, 631−637.

(7) Kanamori, Y.; Iwasaki, A.; Sumimoto, S.; Suenaga, K. *Tetrahedron Lett.* **2016**, *57*, 4213−4216.

(8) (a) Taori, K.; Matthew, S.; Rocca, J. R.; Paul, V. J.; Luesch, H. *J. Nat. Prod.* **2007**, *70*, 1593−1600. (b) Kwan, J. C.; Taori, K.; Paul, V. J.; Luesch, H. *Mar. Drugs* **2009**, *7*, 528−538.

(9) Miller, B.; Friedman, A. J.; Choi, H.; Hogan, J.; McCammon, J. A.; Hook, V.; Gerwick, W. H. *J. Nat. Prod.* **2014**, *77*, 92−99.

(10) (a) Kwan, J. C.; Eksioglu, E. A.; Liu, C.; Paul, V. J.; Luesch, H. *J. Med. Chem.* **2009**, *52*, 5732−5747. (b) Al-Awadhi, F. H.; Law, B. K.; Paul, V. J.; Luesch, H. *J. Nat. Prod.* **2017**, *80*, 2969−2986.

(11) Koblinskia, J. E.; Ahrama, M.; Sloane, B. F. *Clin. Chim. Acta* **2000**, *291*, 113−135.

(12) Strooper, B. D. *Physiol. Rev.* **2010**, *90*, 465−494.

(13) Brik, A.; Wong, C. H. *Org. Biomol. Chem.* **2003**, *1*, 5−14.

(14) The reaction was achieved under the same conditions (0.5 M NaOH− MeOH, 1:1, rt) as for the basic hydrolysis of grassystatin A.[9]

(15) Ohtani, I.; Kusumi, T.; Kashman, Y.; Kakisawa, H. *J. Am. Chem. Soc.* **1991**, *113*, 4092−4096.

(16) Preciado, A.; Williams, P. G. *J. Org. Chem.* **2008**, *73*, 9228−9234.

(17) The exact position of epimerization in the (*S*)-MTPA ester could not be identified because of the scarcity of the samples. We assumed that the epimerization could occur at other acylated oxymethines, C-35 or C-41.

(18) (a) Williams, P. G.; Yoshida, W. Y.; Moore, R. E.; Paul, V. J. *J. Nat. Prod.* **2003**, *66*, 1006−1009. (b) Sun, T.; Zhang, W.; Zong, C.; Wang, P.; Li, Y. *J. Pept. Sci.* **2010**, *16*, 364−374. (c) Al-Awadhi, F. H.; Ratnayake, R.; Paul, V. J.; Luesch, H. *Bioorg. Med. Chem.* **2016**, *24*, 3276−3282.

(19) (a) Morishima, H.; Takita, T.; Aoyagi, T.; Takeuchi, T.; Umezawa, H. *J. Antibiot.* **1970**, *23*, 263−265. (b) Umezawa, H.; Aoyagi, T.; Morishima, H.; Matsuzaki, M.; Hamada, M.; Takeuchi, T. *J. Antibiot.* **1970**, *23*, 259−262.

(20) Baldwin, E. T.; Bhat, T. N.; Gulnik, S.; Hosur, M. V.; Sowder, R. C.; Cachau, R. E.; Collins, J.; Silva, A. M.; Erickson, J. W. *Proc. Natl. Acad. Sci. U. S. A.* **1993**, *90*, 6796−6800.

(21) Benesa, P.; Vetvickab, V.; Fusekc, M. *Crit. Rev. Oncol Hematol* **2008**, *68*, 12−28.

(22) Matarrese, P.; Nencioni, L.; Checconi, P.; Ciarlo, L.; Gambardella, L.; Ascione, B.; Sgarbanti, R.; Garaci, E.; Malorni, W.; Palamara, A. T. *J. Cell. Physiol.* **2011**, *226*, 3368−3377.

(23) *MacroModel*; Schrödinger LLC, New York, NY, 2017.

(24) Pringsheim, E. G. *Pure Cultures of Algae*; Cambridge University Press: London, 1949.

(25) Nübel, U.; Garcia-Pichel, F.; Muyzer, G. *Appl. Environ. Microbiol.* **1997**, *63*, 3327−3332.

(26) Taton, A.; Grubisic, S.; Brambilla, E.; Wit, R. D.; Wilmotte, A. *Appl. Environ. Microbiol.* **2003**, *69*, 5157−5169.

(27) Murakami, A.; Miyashita, H.; Iseki, M.; Adachi, K.; Mimuro, M. *Science* **2004**, *303*, 1633.

(28) Komárek, J.; Anagnostidis, K. In *Suesswasserflora von Mitteleuropa, Bd. 19/2: Cyanoprokaryota: Bd. 2/Part 2: Oscillatoriales*; Spektrum Akademischer Verlag: Stuttgart, 2008.

(29) Engene, N.; Paul, V. J.; Byrum, T.; Gerwick, W. H.; Thor, A.; Ellisman, M. H. *J. Phycol.* **2013**, *49*, 1095−1106.

(30) Engene, N.; Rottacker, E. C.; Kaštovský, J.; Byrum, T.; Choi, H.; Ellisman, M. H.; Komárek, J.; Gerwick, W. H. *Int. J. Syst. Evol. Microbiol.* **2012**, *62*, 1171−1178.

(31) Engene, N.; Tronholm, A.; Salvador-Reyes, L. A.; Luesch, H.; Paul, V. J. *J. Phycol.* **2015**, *51*, 670−681.

(32) Kumar, S.; Stecher, G.; Tamura, K. *Mol. Biol. Evol.* **2016**, *33*, 1870−1874.

(33) Darriba, D.; Taboada, G. L.; Doallo, R.; Posada, D. *Nat. Methods* **2012**, *9*, 772.

(34) Guindon, S.; Gascuel, O. *Syst. Biol.* **2003**, *52*, 696−704.

(35) Stamatakis, A. *Bioinformatics* **2014**, *30*, 1312−1313.

(36) Perrière, G.; Gouy, M. *Biochimie* **1996**, *78*, 364−369.

(37) Ronquist, F.; Teslenko, M.; van der Mark, P.; Ayres, D. L.; Darling, A.; Höhna, S.; Larget, B.; Liu, L.; Suchard, M. A.; Huelsenbeck, J. P. *Syst. Biol.* **2012**, *61*, 539−542.

DOI: 10.1021/acs.jnatprod.8b00417
J. Nat. Prod. XXXX, XXX, XXX−XXX